Research article

Ki Young Lee, Kwang Wook Yoo, Youngsun Choi, Gunpyo Kim, Sangmo Cheon,
Jae Woong Yoon* and Seok Ho Song*

Topological guided-mode resonances at non-Hermitian nanophotonic interfaces

Abstract: The topological properties of photonic microstructures are of great interest because of their experimental feasibility for fundamental study and potential applications. Here, we show that robust guided-mode-resonance states exist in photonic domain-wall structures whenever the complex photonic band structures involve certain topological correlations in general. Using the non-Hermitian photonic analogy of the one-dimensional Dirac equation, we derive essential conditions for photonic Jackiw-Rebbi-state resonances taking advantage of unique spatial confinement and spot-like spectral features which are remarkably robust against random parametric errors. Therefore, the proposed resonance configuration potentially provides a powerful method to create compact and stable photonic resonators for various applications in practice.

Keywords: guided-mode resonance; non-Hermitian effect; subwavelength grating; topological effect.

1 Introduction

Non-Hermitian and topological properties in photonic structures attract considerable attention as they are related to exotic optical phenomena resulting from the parity-time symmetry and topological interaction properties. Such phenomena include wave dynamics related to half-integer topological invariants at exceptional-point

singularities [1], topological phase transition in complex photonic band structures [2], and polarization vortices around optical bound states in the continuum (BIC) [3, 4], to mention a few. Intriguingly, extra degrees of freedom in non-Hermitian systems and parametric insusceptibility of topological effects potentially provide powerful means for versatile and robust control schemes against various environmental disturbances, detrimental performance drift, and uncontrollable errors in practice.

Toward this end, we notice topological interface states [5] as an operative discrete state for robust guided-mode-resonance (GMR) effects [6–9] that might significantly alleviate practical limitations in the conventional approaches. For instance, narrow-band planar GMR elements have a fundamental lower limit in their transversal footprint size D in 100-μm or mm scales [10, 11] because of in-plane propagation of operative modes within their lifetime in the order of 10^2–10^4 optical cycles. Although D can be significantly reduced by including additionally distributed Bragg-reflection lattices at the device boundary areas [12], the additional reflector components not only occupy inactive surplus areas but also increase additional complications in design and fabrication. Therefore, the fundamental size limit significantly restricts potential applications in which high-density integration is required.

In another consideration, a GMR appears on a characteristic dispersion curve extended over a broad frequency band in general. Consequently, spectral loci of GMRs change with variation in the angle of incidence or with spatial drift of lattice's geometrical parameters unavoidably included as fabrication imperfections. Associated technical issues are the high sensitivity of the excitation efficiency to optical alignment, thermo-optic drift of intensity and phase, and inhomogeneous broadening of the spectral resonance features for poorly collimated or spatially wide excitation-light beams.

Importantly, GMRs by topological interface states are potentially free from the conventional footprint-size limitation and technical issues resulting from characteristic dispersion bands because they are essentially confined in

*Corresponding authors: Jae Woong Yoon and Seok Ho Song,
Department of Physics, Hanyang University, Seoul, 04763, Korea,
E-mail: yoonjw@hanyang.ac.kr (J.W. Yoon), shsong@hanyang.ac.kr
(S.H. Song). https://orcid.org/0000-0002-3362-6873 (J.W. Yoon)
**Ki Young Lee, Kwang Wook Yoo, Youngsun Choi, Gunpyo Kim
and Sangmo Cheon,** Department of Physics, Hanyang University,
Seoul, 04763, Korea

both vertical and lateral axes and, thereby, their spectral features appear at discrete frequency levels, not over extended frequency bands. In this paper, we theoretically show that such a topological GMR state indeed exists at an interface between two different thin-film photonic lattices whenever certain topological correlations in the complex photonic band structures are included in general. Using a photonic analogy of the 1D Dirac equation for relativistic elementary particles, we derive essential conditions for a photonic Jackiw-Rebbi state [13, 14] that produces strong lateral confinement and desired spot-like spectral GMR feature in the wavevector-frequency domain.

Previously, the optical analogy of the Jackiw-Rebbi states and associated phenomena have been studied in various structures including channel waveguide arrays [15], coupled ring-resonator optical waveguides [16], magneto-electric Mie-resonance particle chains [17], and polaritonic micro-cavity lattices [18, 19]. In these structures, desired topological coupling configurations are directly coded in optical synthetic atoms by means of inter-atom interactions of electromagnetic wave functions localized in the explicit position-space domain. In our GMR configurations, in contrast, each grating ridges do not operate as synthetic atoms accommodating localized photonic wave functions. Instead, they provide desired coupling configurations between delocalized guided-mode

wave functions in terms of discrete diffraction orders in the implicit wavevector domain. Therefore, our approach suggests further opportunity of the topological phenomena over broad classes of diffractive optical systems on which numerous practical applications are grounded. Along this line, we present formal consistency between the diffractive coupled-mode theory of guided-mode resonances and elementary topological band theory of electrons. The calculated confinement length of this topological GMR suggests the possibility of overcoming the fundamental lower limit of the device footprint size in conventional planar GMR elements. In addition, we show remarkable stability of this topological GMR effect against random parametric errors in the lattice's structure geometry.

2 Topological guided-mode resonance

Introducing a photonic analogy of the 1D Dirac equation and associated topological resonance states, we consider a simple 1D dielectric grating in the zero-order regime below the Rayleigh frequency, as schematically illustrated in Figure 1(a). The structure is defined in terms of period Λ, thickness d, fill factor F, and dielectric constants ε_c for
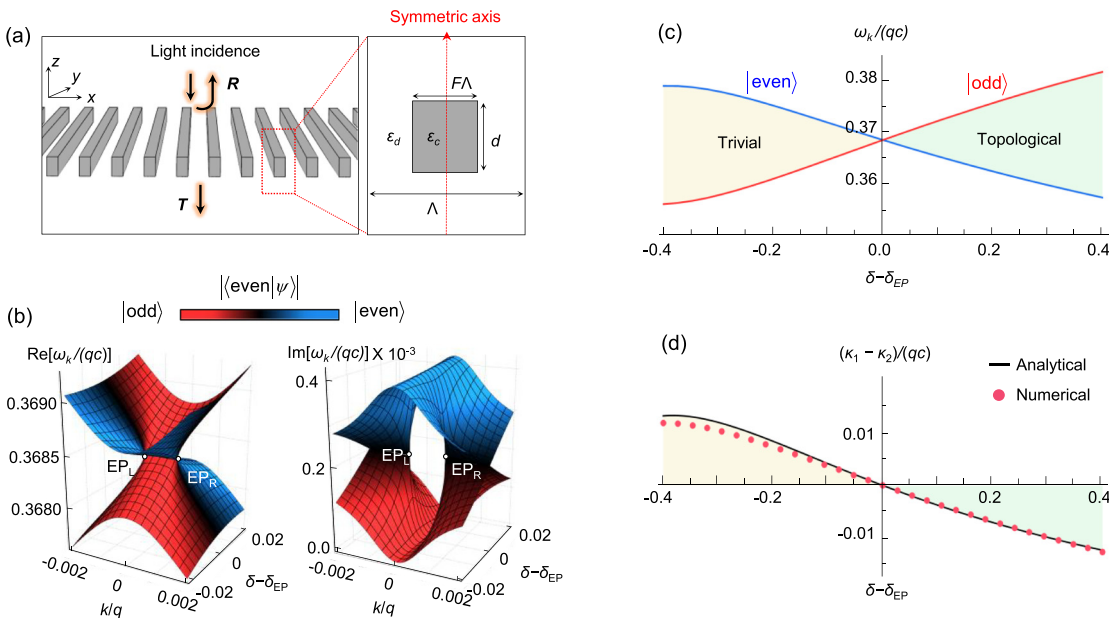

Figure 1: Non-Hermitian topological properties of a second-order guided-mode resonance grating.
(a) Schematic of a thin-film guided-mode-resonance grating. (b) The transition of the real and imaginary frequency bands by Eqs. (5) and (6) as topology-tuning parameter δ changes. A pair of exceptional points are indicated by EP_L and EP_R. Skin color indicates relative even-mode strength $|\langle even|\psi\rangle|$ for the corresponding eigenstate. (c) Band-edge frequency change as a function of δ by the FEM method. (d) Coupling rate $\kappa_1 - \kappa_2$ as a function of δ by the analytic theory in comparison with the numerical analysis (FEM method).

high-index bars and ε_d ($<\varepsilon_c$) for the surrounding medium. Therefore, the structure can be conveniently represented by a periodic dielectric function

$$\epsilon(x,z) = \sum_m \epsilon_m(z)e^{imqx} \tag{1}$$

with z-dependent Fourier-series coefficient $\varepsilon_m(z)$ and grating vector $q = 2\pi\Lambda^{-1}$. Describing transverse-electric (TE) guided-mode-resonance (GMR) states in this structure, we solve a planar electromagnetic wave equation

$$\left[\frac{\partial^2}{\partial x^2} + \frac{\partial^2}{\partial z^2} + \frac{\omega_k^2}{c^2}\epsilon(x,z)\right]E_k(x,z) = 0 \tag{2}$$

for electric-field amplitude E_k taking a modal expansion

$$\begin{aligned}E_k = \{&L(z) + [\psi_s\sin(qx + \phi_0) \\ &+ \psi_c\cos(qx + \phi_0)]u(z)\}e^{ikx},\end{aligned} \tag{3}$$

where k is Bloch wavevector, $L(z)$ is leakage-radiation amplitude, $\psi_{s\text{ or }c}$ is the amplitude of the periodic guided modes, and ϕ_0 is a phase constant. Guided-mode wave function $u(z)$ is determined by a wave equation

$$\left[\frac{\partial^2}{\partial z^2} + \frac{\omega^2}{c^2}\epsilon_0(z)\right]u(z) = \beta^2 u(z), \tag{4}$$

where β denotes propagation constant of the guided mode on a characteristic dispersion relation $\omega = \omega_u(\pm\beta)$.

Solving Eq. (2) with the modal expansion in Eq. (3), we consider a restricted domain $k \ll q$ near the second-order stop band $\omega_k \approx \omega_q = \omega_u(q)$ and assume that guided-mode amplitudes ψ_s and ψ_c take significant values if phase matching condition $k \pm q = \pm\beta$ is satisfied, in the same manner as the coupled-mode theory by Kazarinov and Henry [2, 20–22]. In an approximation taking the lowest-order diffraction coupling between the forward and backward guided modes into account under such conditions, Eq. (2) reduces to a non-Hermitian matrix eigenvalue problem

$$\mathbf{H}_{\text{GMR}}|\psi\rangle = (E - i\Delta)|\psi\rangle \tag{5}$$

with $|\psi\rangle$ representing a column vector $[\psi_s \; \psi_c]^T$. Here, Hamiltonian $\mathbf{H}_{\text{GMR}}$ is given by

$$\mathbf{H}_{\text{GMR}} = (\kappa_1 - \kappa_2 + i\gamma)\boldsymbol{\sigma}_x - kv_g\boldsymbol{\sigma}_y, \tag{6}$$

where $\boldsymbol{\sigma}_j$ is the Pauli matrix, $v_g = [\partial\omega_u/\partial\beta]_{\beta=q}$ denotes group speed of the guided mode at $\omega = \omega_q$, κ_1 represents coupling rate between the forward and backward guided modes through two consecutive first-order diffraction processes, κ_2 represents coupling rate between the forward and backward guided modes through one second-order diffraction process, and γ represents leakage-radiation

rate of the uncoupled guided mode. The initial phase constant ϕ_0 is chosen such that $\phi_0 = \pi/4 - qx_0$ with x_0 denoting x position of the structure's mirror-symmetry plane. The complex eigenvalue $E - i\Delta$ in Eq. (5) is defined to represent resonance frequency $\Omega = \text{Re}(\omega_k) = \omega_q + \kappa_1 + E$ and decay rate $\Gamma = -\text{Im}(\omega_k) = \gamma + \Delta$. See Supplementary Material for detailed mathematical treatment.

$\mathbf{H}_{\text{GMR}}$ describes resonance states near the second-order Bragg condition and their frequency bands in terms of its eigenvalues and eigenvectors. For example, the eigenvalues and corresponding eigenvectors at $k = 0$ are determined by

$$E_\pm - i\Delta_\pm = \pm p_{12}(\kappa_1 - \kappa_2 + i\gamma), \tag{7}$$

$$|\psi_\pm\rangle = \frac{1}{\sqrt{2}}\begin{bmatrix} 1 \\ \pm p_{12} \end{bmatrix}, \tag{8}$$

where p_{12} is signum function $\text{sgn}(\kappa_1 - \kappa_2)$, i.e., $p_{12} = +1$ for $\kappa_1 - \kappa_2 > 0$ whereas $p_{12} = -1$ for $\kappa_1 - \kappa_2 < 0$. It immediately follows that upper band-edge frequency $\Omega_2 = \omega_q + \kappa_1 + |\kappa_1 - \kappa_2|$ and lower band-edge frequency $\Omega_1 = \omega_q + \kappa_1 - |\kappa_1 - \kappa_2|$. The corresponding eigenvectors and leakage-radiation rates are determined differently depending on p_{12}. For $p_{12} = +1$, i.e., $\kappa_1 - \kappa_2 > 0$, $|\psi_+\rangle$ takes super-radiant state $|\text{even}\rangle = 2^{-1/2}[1\ 1]^T$ with radiation decay rate $\Gamma_+ = 2\gamma$ at upper band-edge Ω_2 whereas $|\psi_-\rangle$ takes sub-radiant state $|\text{odd}\rangle = 2^{-1/2}[1\ {-1}]^T$ with radiation decay rate $\Gamma_- = 0$ at lower band-edge Ω_1. We note that super-radiant and sub-radiant states correspond to the leaky GMR and BIC, respectively, in common terminology. For $p_{12} = -1$, i.e., $\kappa_1 - \kappa_2 < 0$, in contrast, $|\psi_+\rangle = |\text{odd}\rangle$ with $\Gamma_+ = 0$ at upper band-edge Ω_2 whereas $|\psi_-\rangle = |\text{even}\rangle$ with $\Gamma_- = 2\gamma$ at lower band-edge Ω_1. This frequency flip between the super-radiant and sub-radiant states is understood as resulting from the change in Bragg-reflection phase from 0 to π in response to the sign flip in $\kappa_1 - \kappa_2$ value [2].

Importantly, the band-edge state flip depending on $\text{sgn}(\kappa_1 - \kappa_2)$ in our theory reveals topological properties of waveguide-grating structures in the second-order Bragg-reflection regime. $\mathbf{H}_{\text{GMR}}$ in Eq. (6) is formally identical to a bulk momentum-space Su-Schrieffer-Heeger (SSH) Hamiltonian $\mathbf{H}_{\text{SSH}} = (w - v)\boldsymbol{\sigma}_x - vk\Lambda\boldsymbol{\sigma}_y$ in the low-energy continuum approximation for a 1D dimer chain, where v is intra-cell coupling rate and w is inter-cell coupling rate [23]. ψ_s and ψ_c in state vector $|\psi\rangle$ represent amplitudes of two independent standing guided modes $u(z)\sin[q(x - x_0) + \pi/4]$ and $u(z)\cos[q(x - x_0) + \pi/4]$ in analogy to the right and left site excitations in a 1D-periodic dimer chain. Therefore, we can intuitively understand topological properties of second-order GMR gratings in direct analogy to the 1D SSH model by taking a parametric parallelism $w - v = \kappa_1 - \kappa_2 + i\gamma$ and $v = \Lambda^{-1}v_g$.

The topological phase of a lattice in the SSH model is determined by $\text{sgn}(w - v)$ such that the lattice is in the trivial phase for $\text{sgn}(w - v) = +1$ or in the topological phase for $\text{sgn}(w - v) = -1$. A geometrical phase referred to as the Zak phase for the energy band takes π in the topological phase or 0 otherwise [23, 24]. The nonzero Zak phase implies that spatial symmetry of the eigenvector gradually changes within the associated energy band and it also indicates the existence of an edge-confined state in the middle of the energy bandgap, which explains surface electric conduction in topological insulators. Taking the parametric parallelism between $\mathbf{H}_{\text{SSH}}$ and $\mathbf{H}_{\text{GMR}}$ into account, such topological properties in second-order GMR gratings appear when $\text{sgn}(\kappa_1 - \kappa_2) = -1$ for the topological phase and $\text{sgn}(\kappa_1 - \kappa_2) = +1$ for the trivial phase.

Confirming the topological transition of a second-order GMR grating depending on $\text{sgn}(\kappa_1 - \kappa_2)$, we provide complex-frequency band structure, spatial-symmetry of the photonic eigenvector $|\psi\rangle$, and key parameters depending on topology-adjusting parameter δ, as shown in Figure 1(b)–(d). δ is defined such that refractive index of the grating bars $n_c = n_d + \delta$ with $n_d = \varepsilon_d^{1/2}$ denoting refractive index of the surrounding medium and fill factor $F = (n_c - n_d)/(2\delta)$. Following these specific rules for fill factor F and refractive index n_c with respect to δ, second-order Bragg-reflection frequency ω_q is kept nearly constant whereas δ is changing over distinguished ranges of $\delta < \delta_{\text{EP}}$ in the trivial phase ($\kappa_1 - \kappa_2 > 0$), $\delta = \delta_{\text{EP}}$ at the critical point ($\kappa_1 - \kappa_2 = 0$), and $\delta > \delta_{\text{EP}}$ in the topological phase ($\kappa_1 - \kappa_2 < 0$). $\delta_{\text{EP}} = 1.035$ for the critical point in our case with $n_d = 2.45$. We use the finite-element method for this numerical analysis.

In the complex-frequency band structures in Figure 1(b), the real-frequency bands and associated spatial symmetry of the resonance modes show drastic transitions with respect to the critical point at $\delta = \delta_{\text{EP}}$ where $\kappa_1 - \kappa_2 = 0$. The band-edge state flip between $|\text{even}\rangle$ and $|\text{odd}\rangle$ is clearly visible from the skin-color transition between blue to red as δ increases from the trivial-phase region ($\delta < \delta_{\text{EP}}$) to the topological-phase region ($\delta > \delta_{\text{EP}}$). For the critical point at $\delta = \delta_{\text{EP}}$, the real and imaginary frequency bands show self-intersecting Riemann-surface geometries near two exceptional points (EP), instead of having a Dirac point, as a result of the non-Hermiticity induced by nonzero radiation decay ($\gamma > 0$). We note that the EPs at the critical point are inevitable for the second-order GMRs for which radiation decay cannot be completely eliminated as far as they appear within the spectral domain for the external radiation continuum. Figure 1(c) and (d) show transition of the band-edge frequencies for $|\text{even}\rangle$ and $|\text{odd}\rangle$ as functions of δ in

association with the change in $\kappa_1 - \kappa_2$ as the key topological parameter.

Associated with such topological properties, a junction of two topologically distinguished lattices supports an interface-localized state known as the Jackiw-Rebbi state [13]. A Jackiw-Rebbi state is derived from the 1D Dirac equation as

$$\mathbf{H}_{\text{Dirac}}|\psi_D\rangle = E_D|\psi_D\rangle, \tag{9}$$

$$\mathbf{H}_{\text{Dirac}} = mc^2\boldsymbol{\sigma}_z - pc\boldsymbol{\sigma}_x, \tag{10}$$

where m and p are Dirac mass and momentum of the basic state, respectively, and c is the speed of light in vacuum. For a Dirac mass distribution given by $m(x) = -m_L\alpha(-x) + m_R\alpha(x)$ ($m_L > 0$ and $m_R > 0$), where $\alpha(x)$ is the Heaviside step function, the 1D Dirac equation allows an interface-localized eigenstate as

$$|\psi_D\rangle = \sqrt{\frac{c}{\hbar}\frac{m_L m_R}{m_L + m_R}}e^{-|m(x)cx|/\hbar}\begin{bmatrix} 1 \\ i \end{bmatrix} \tag{11}$$

at $p = 0$ and $E_D = 0$. This state is a 1D Jackiw-Rebbi state at an interface between two spaces with negative and positive Dirac masses, respectively.

This type of Jakiw-Rebbi state can be excited at a photonic interface between two GMR gratings with different topological phases as there is an exact isomorphism between $\mathbf{H}_{\text{Dirac}}$ and $\mathbf{H}_{\text{GMR}}$ with unitary transformation $\mathbf{U} = 2^{-1}(\boldsymbol{\sigma}_0 - i\boldsymbol{\sigma}_x + i\boldsymbol{\sigma}_y - i\boldsymbol{\sigma}_z)$, i.e., $\mathbf{U}\mathbf{H}_{\text{GMR}}\mathbf{U}^\dagger = \mathbf{H}_{\text{Dirac}}$ with a parametric parallelism

$$p = \hbar k, c = v_g, \text{ and } m = \hbar(\kappa_1 - \kappa_2 + i\gamma)v_g^{-2} \tag{12}$$

We notice here that the real part of Dirac mass m is determined by $\kappa_1 - \kappa_2$ and the unitary transformation preserves the eigenvalue spectrum and the surface-localized norm in Eq. (11) as well. Therefore, a Jakiw-Rebbi state in Eq. (11) must exist at $k = 0$ and $E - i\Delta = E_D = 0$, i.e., frequency $\Omega = \omega_q + \kappa_1 \approx \omega_q$ and decay rate $\Gamma = \gamma$, for a photonic interface between two second-order GMR gratings, one in the trivial phase and the other in the topological phase. Under this unitary transformation, Dirac-equation state vector $|\psi_D\rangle = \mathbf{U}|\psi\rangle$ is interpreted as representing amplitudes of two standing guided modes $u(z)\sin[q(x - x_0)]$ and $u(z)\cos[q(x - x_0)]$. Note that these basis wave functions for the 1D Dirac equation respectively correspond to $|\text{odd}\rangle$ and $|\text{even}\rangle$ in the GMR eigenvalue problem in Eq. (5).

We numerically demonstrate the photonic Jackiw-Rebbi state at an interface between two second-order GMR gratings as shown in Figure 2. Therein, we assume $m_L = m_R = 0.01$ for an analytic solution because of Eq. (11) and corresponding GMR gratings for a numerical solution
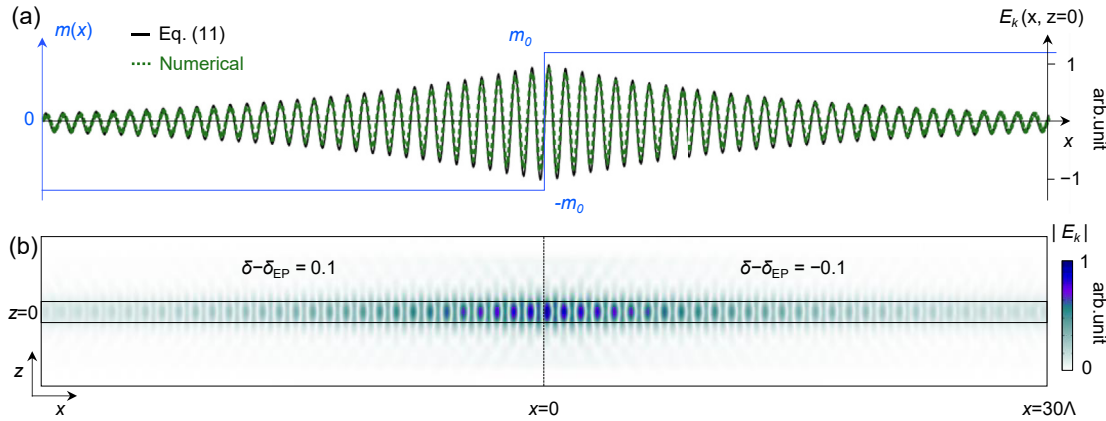
Figure 2. Leaky Jackiw-Rebbi state at a photonic topological interface.
(a) Cross-sectional field profile of a leaky photonic Jackiw-Rebbi state in comparison with the analytic solution in Eq. (11). (b) The two-dimensional field pattern of a leaky photonic Jackiw-Rebbi state.

by the FEM method have $\delta = \delta_{EP} + 0.1$ on the left side and $\delta = \delta_{EP} - 0.1$ on the right side of the interface, according to the parametric correspondence in Eq. (12). This parameter set corresponds to $\{n_c = 3.385, F = 0.442\}$ for $\delta = -0.1$ and $\{n_c = 3.585, F = 0.365\}$ for $\delta = +0.1$. Quantitative agreement between two independent solutions confirms the existence of the leaky Jackiw-Rebbi state. The field-intensity pattern in Figure 2(b) shows the localization of this state in both vertical and lateral axes. In particular, the lateral confinement because of the topological properties is characterized by confinement length $L_c = \hbar|mc|^{-1} = v_g|\kappa_1 - \kappa_2|^{-1}$ according to Eqs. (11) and (12). L_c is favorably adjustable by tuning $|\kappa_1 - \kappa_2|$ with grating fill factor and thickness controls in principle. Therefore, the photonic Jackiw-Rebbi state in second-order GMR gratings can be considered as a promising guided-mode resonance state

which is localized in space, frequency, and angular domains, as we will show further in the following sections.

3 Resonance properties

In a further study of guided-mode-resonance effects from photonic Jackiw-Rebbi states, we perform rigorous numerical analyses on resonant reflection spectra using the FEM method. Figure 3(a)–(c) are angle-dependent reflection spectra for three different topological conditions: the trivial phase ($\delta = \delta_{EP} - 0.15$), the critical point ($\delta = \delta_{EP}$), and the topological phase ($\delta = \delta_{EP} + 0.15$). They show characteristic spectral features associated with the topological phase transition. For the trivial phase in Figure 3(a), the relatively broad reflection peak at the upper band edge
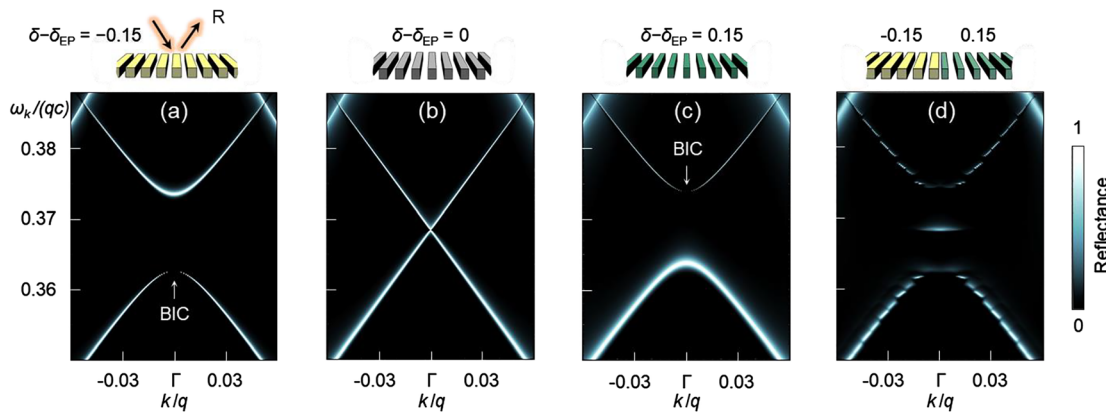

Figure 3: Spectral features of a leaky Jackiw-Rebbi-state resonance on $\omega-k$ plane.
Guided-mode-resonance dispersions in the reflection spectra for (a) the trivial phase, (b) critical point, and (c) topological phase. (d) Photonic leaky Jackiw-Rebbi-state-resonance feature in the reflection spectrum. We assume a topological interface of two guided-mode-resonance gratings with $\delta - \delta_{EP} = -0.15$ and 0.15.

is an indication of resonant excitation of super-radiant state |even⟩ whereas vanishingly narrow reflection peak at the lower band edge is because of the sub-radiant state |odd⟩ excitation, as described in the previous section. This sub-radiant resonance is also referred to as symmetry-protected BIC because of its asymptotically non-radiating property toward the Γ point. At the critical point in Figure 3(b), two guided-mode resonance bands are crossing in analogy to a Dirac point for an effectively massless state. For the topological phase in Figure 3(c), the super-radiant and sub-radiant resonance features flip over their locations each other, as previously studied in [2]. We note therein that the band crossing, EP emergence, and band flip effects associated with the topological phase transition here are explained in terms of superposition of multiple-order Bragg processes using the coupled-mode theory by Kazarinov and Henry [20].

A junction of two GMR gratings for Figure 3(a) and (c) supports a photonic Jackiw-Rebbi state as shown in Figure 3(d). The Jackiw-Rebbi-state resonance appears at the mid-point of the two band edges. As described in the previous section, this topological guided-mode resonance is localized in both frequency and wavevector (or angle of incidence equivalently) domains. Although the resonance bandwidth $\Delta\omega$ in frequency is simply given by $\Delta\omega \approx \gamma$, i.e., the decay rate of an uncoupled guided mode, its resonance bandwidth Δk in wavevector is determined by $\Delta k \approx L_c^{-1}$, i.e., inverse lateral-confinement length and the corresponding angular bandwidth $\Delta\theta$ is $\Delta\theta \approx \lambda(2\pi n_d L_c)^{-1}$, where λ is wavelength in vacuum. We note that this spot-like resonance spectrum is a unique feature which is not obtainable in conventional GMR configurations.

We further study the lateral confinement effect in consideration of miniaturization and field-enhancement capabilities obtainable with the topological GMR by the photonic Jackiw-Rebbi state. In Figure 4(a), we calculate intensity envelope distribution $\langle\psi_D|\psi_D\rangle$ from Eq. (11) depending on $|\delta - \delta_{EP}|$ value. The intensity distributions show stronger confinement for higher $|\delta - \delta_{EP}|$ value, following the dependence of the confinement length $L_c = \hbar|mc|^{-1} = v_g|\kappa_1 - \kappa_2|^{-1}$. In particular, L_c is well within 10Λ for $|\delta - \delta_{EP}| = 0.4$ which corresponds to $L_c < 5\,\mu m$ for $\Lambda \sim 500$ nm and refractive-index contrast $n_c - n_d \sim 0.4$. Field enhancement increases as the confinement get stronger with increasing $|\delta - \delta_{EP}|$, as shown in Figure 4(b). From Eqs. (11) and (12), we see that field enhancement for the photonic Jackiw-Rebbi state scales with a factor $\hbar^{-1}c|m_L m_R(m_L + m_R)^{-1}| = v_g^{-1}|\kappa_1 - \kappa_2| = L_c^{-1}$. We note that this field enhancement by the lateral confinement provides an additional factor to the enhancement by temporal accumulation of incident optical energy during the resonance lifetime.
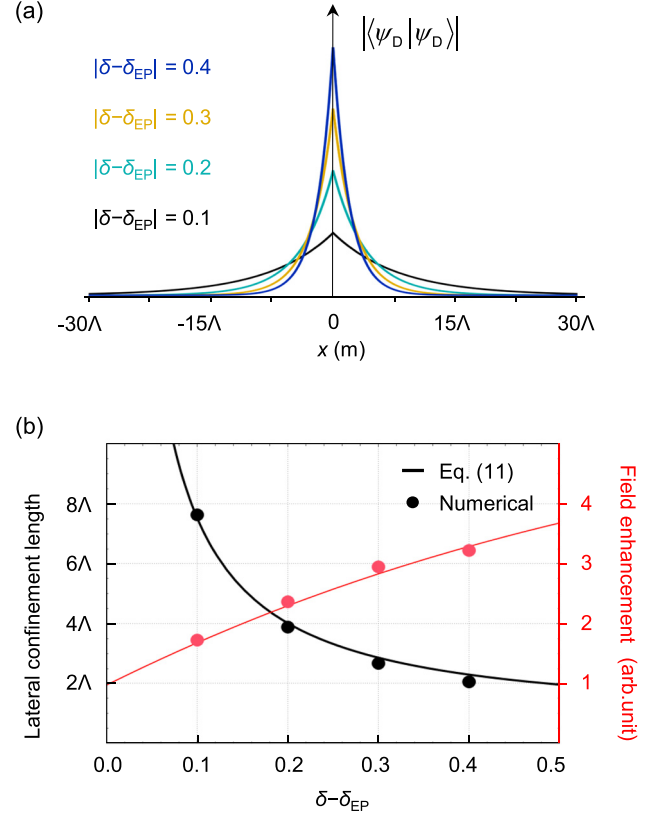

Figure 4: Lateral confinement and subsequent field enhancement of a photonic Jackiw-Rebbi state.
(a) Absolute amplitude profile across the interface as a function of topology-tuning parameter δ. (b) Lateral confinement length and field-enhancement factor at the interface as functions of δ.

Finally, we investigate the robustness of the proposed topological GMR effect against parametric errors which is inevitable in experiments in general. We consider a topological junction of two 50-period Si GMR gratings with identical thickness $d = 500$ nm in Si_3N_4 as the surrounding medium. Fill factors and periods are denoted by $F_{1\,or\,2}$ and $\Lambda_{1\,or\,2}$ and they are subject to random position error $\Delta F(x_n)$ following the Gaussian distribution for a variance at 0.05, as indicated in Figure 5(a) and (b). Figure 5(c) shows the calculated reflection spectra for 20 independent random error distributions in comparison with the ideal case free from these errors. We clearly notice that the impact of the random parametric errors on the resonance location and bandwidth is greatly alleviated for the topological resonance at the center when compared to the two side peaks by the band-edge GMR features which have been mainly used previously. In particular, the resonance-center shift for the topological resonance is only 16% of that for the band-edge resonances on average. Resonance Q-factor change for the topological resonance is also reduced down to 32% of that for the band-edge resonances when
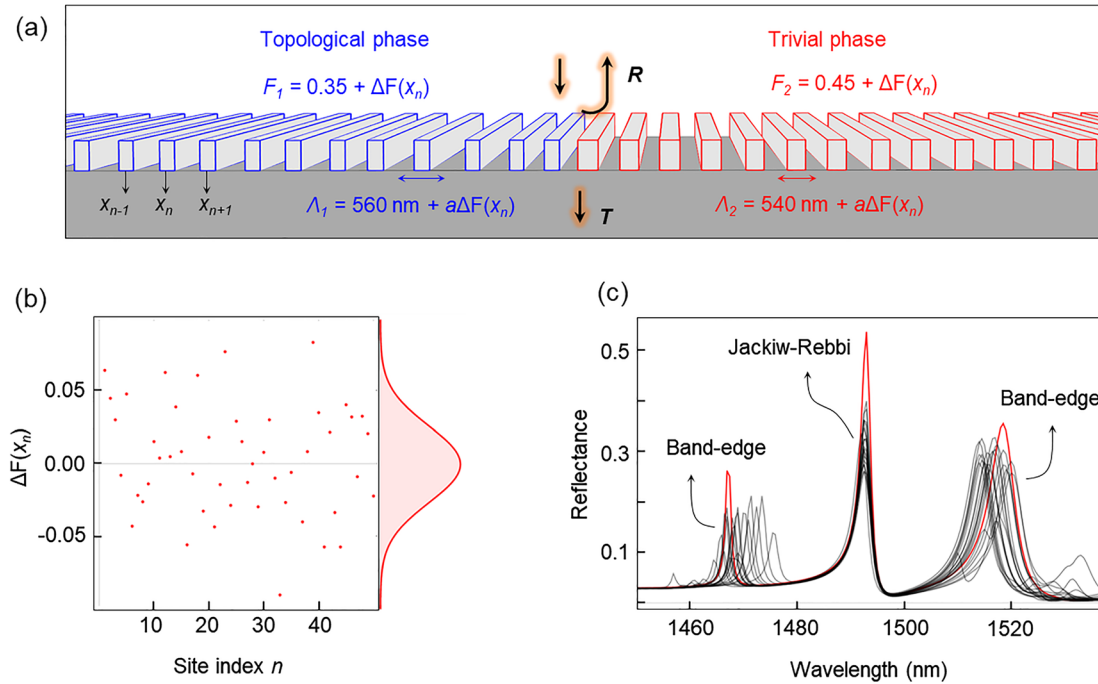
Figure 5: Topological robustness against random structural errors.
(a) Schematic drawing of photonic junction consisting of two different Si-gratings with refractive index $n_1 = 3.485$ in Si_3N_4 with refractive index $n_2 = 2.450$. The two gratings on the left (topological) and right (trivial) have spatially varying fill factors and periods $[F_i, \Lambda_i]$ for each unit-cell position x_n such that $F_1 = 0.35 + \Delta F(x_n)$, $\Lambda_1 = 560$ nm $+ a\Delta F(x_n)$, $F_2 = 0.45 + \Delta F(x_n)$, and $\Lambda_2(x_n) = 540$ nm $+ a\Delta F(x_n)]$ with period-error constant $a = 185$ nm. (b) One sample of the randomly generated error distribution $\Delta(x_n)$ following a Gaussian distribution function for variance 0.05. (c) Calculated reflection spectra with the Gaussian random errors for surface-normal TE incidence. The red curve indicates the error-free ideal case.

compared at their maxima. Therefore, the proposed topological GMR has highly favorable characteristics in device foot-print size, field enhancement, and spectral precision for various applications in practice.

Considering possible modulation instability with respect to resonance center position and bandwidth, relevant factors should be refractive indices of constituent materials, average period, and lateral size of the entire structure. Change in refractive indices or average period directly affects resonance position because they change propagation constant of guide modes or Bragg condition, respectively, and lead to the overall shift of the dispersion bands. Associated with such changes in the resonance position, mismatch in the mid-gap positions between two GMR gratings forming a topological junction may cause a detrimental impact on the existence of the topological GMR states. In particular, the photonic Jackiw-Rebbi state persistently exists as far as the mid-gap-position mismatch is limited within the stop-band overlap region. See Supplementary Material for details. Size reduction within the lateral-confinement length causes a substantial increase in the resonance bandwidth since leakage radiation

toward the side edges becomes significant, as previously treated in [25] for purely 1D scattering systems.

4 Conclusion

Incorporating a non-Hermitian photonic analogy of the 1D Dirac equation for relativistic particles, we have developed a comprehensive theory of topological guided-mode resonance states in thin-film photonic lattice structures coupling with external radiation continuum. The theory predicts topological GMR states in the complex frequency domain and its unique spatial and spectral characteristics which are robust against random parametric errors. In particular, the unique spot-like resonance feature in the frequency-wavevector domain provides a well-defined discrete angular and spectral channel in contrast to the conventional GMR structures having continuous resonance bands which are often problematic in precise filter applications. In addition, the lateral confinement and subsequent field enhancement potentially enable compact

and integration-compatible device configurations without any loss in the resonance Q factor. Importantly, these properties are topologically protected against random parametric errors at significant magnitude. Therefore, the proposed topological GMR is favorable for various applications such as optical filters, bio-chemical sensor templates, surface-emitting lasers, and fundamental study on non-Hermitian topological physics as well.

References

[1] H. Zhou, C. Peng, Y. Yoon, et al., "Observation of bulk Fermi arc and polarization half charge from paired exceptional points," *Science*, vol. 359, p. 6379, 2018.

[2] S. Lee and S. R. Magnusson, "Band flips and bound-state transitions in leaky-mode photonic lattices," *Phys. Rev. B*, vol. 99, p. 045304, 2019.

[3] B. Zhen, C. W. Hsu, L. Lu, A. D. Stone, and M. Soljačić, "Topological nature of optical bound states in the continuum," *Phys. Rev. Lett.*, vol. 113, p. 257401, 2014.

[4] H. M. Doeleman, F. Monticone, W. den Hollander, A. Alù, and A. F. Koenderink, "Experimental observation of a polarization vortex at an optical bound state in the continuum," *Nat. Photonics*, vol. 12, p. 397, 2018.

[5] Y. Lumer, Y. Plotnik, M. C. Rechtsman, and M. Segev, "Self-localized states in photonic topological insulators," *Phys. Rev. Lett.*, vol. 111, p. 243905, 2013.

[6] J. Jin, X. Yin, L. Ni, M. Soljačić, B. Zhen, and C. Peng, "Topologically enabled ultrahigh-Q guided resonances robust to out-of-plane scattering," *Nature*, vol. 574, p. 7779, 2019.

[7] L. H. Wu and X. Hu, "Scheme for achieving a topological photonic crystal by using dielectric material," *Phys. Rev. Lett.*, vol. 114, p. 223901, 2015.

[8] A. B. Khanikaev and G. Shvets, "Two-dimensional topological photonics," *Nat. Photonics*, vol. 11, p. 763, 2017.

[9] T. Ozawa, H. M. Price, A. Amo, et al., "Topological photonics," *Rev. Mod. Phys.*, vol. 91, p. 015006, 2019.

[10] R. R. Boye and R. K. Kostuk, "Investigation of the effect of finite grating size on the performance of guided-mode resonance filters," *Appl. Opt.*, vol. 39, p. 3649, 2020.

[11] J. Lee, B. Zhen, S. L. Chua, et al., "Observation and differentiation of unique high-Q optical resonances near zero wave vector in macroscopic photonic crystal slabs," *Phys. Rev. Lett.*, vol. 109, p. 067401, 2012.

[12] K. Kintaka, K. Asai, K. Yamada, J. Inoue, and S. Ura, "Grating-position-shifted cavity-resonator-integrated guided-mode resonance filter," *IEEE Photonics Technol. Lett.*, vol. 29, p. 201, 2017.

[13] R. Jackiw and C. Rebbi, "Solitons with fermion number ½," *Phys. Rev. D*, vol. 13, p. 3398, 1976.

[14] S. Q. Shen, *Topological Insulators*, Berlin, Springer, 2012.

[15] T. X. Tran, H. M. Nguyen, and D. C. Duong, "Jackiw-Rebbi states in interfaced binary waveguide arrays with Kerr nonlinearity," *Phys. Rev. A*, vol. 100, p. 053849, 2019.

[16] S. Mittal, J. Fan, S. Faez, A. Migdall, J. M. Taylor, and M. Hafezi, "Topologically robust transport of photons in a synthetic gauge field," *Phys. Rev. Lett.*, vol. 113, p. 087403, 2014.

[17] A. A. Gorlach, D. V. Zhirihin, A. P Slobozhanyuk, A. B. Khanikaev, and M. A. Gorlach, "Photonic Jackiw-Rebbi states in all-dielectric structures controlled by bianisotropy," *Phys. Rev. B*, vol. 99, p. 205122, 2019.

[18] T. Ozawa, A. Amo, J. Bloch, and I. Carusotto, "Klein tunneling in driven-dissipative photonic graphene," *Phys. Rev. A*, vol. 96, p. 013813, 2017.

[19] T. Jacqmin, I. Carusotto, I. Sagnes, et al., "Direct observation of Dirac cones and a flatband in a honeycomb lattice for polaritons," *Phys. Rev. Lett.*, vol. 112, p. 116402, 2014.

[20] R. F. Kazarinov and C. H. Henry, "Second-order distributed feedback lasers with mode selection provided by first-order radiation losses," *IEEE J. Quant. Electron.*, vol. 21, p. 144, 1985.

[21] D. Rosenblatt, A. Sharon, and A. A. Friesem, "Resonant grating waveguide structures," *IEEE J. Quant. Electron.*, vol. 33, p. 11, 1997.

[22] Y. Ding and R. Magnusson, "Band gaps and leaky-wave effects in resonant photonic-crystal waveguides," *Opt. Express*, vol. 15, p. 2, 2007.

[23] S. Lieu, "Topological phases in the non-Hermitian Su-Schrieffer-Heeger model," *Phys. Rev. B*, vol. 97, p. 045106, 2018.

[24] J. Zak, "Berry's phase for energy bands in solids," *Phys. Rev. Lett.*, vol. 62, p. 2747, 1989.

[25] P. A. Kalozoumis, G. Theocharis, V. Achilleos, S. Félix, O. Richoux, and V. Pagneux, "Finite-size effects on topological interface states in one-dimensional scattering systems," *Phys. Rev. A*, vol. 98, p. 023838, 2018.